

Supporting Information

Real-Time Discrimination and Versatile Profiling of Spontaneous ROS in Living

Organisms with a Single Fluorescent Probe

Ruilong Zhang,^{a,b,†} Jun Zhao,^{a,†} Guangmei Han,^{a,†} Zhengjie Liu,^{a,b} Cui Liu,^{a,b} Cheng Zhang,^{a,b}
Bianhua Liu,^a Changlong Jiang,^a Renyong Liu,^a Tingting Zhao,^a Ming-Yong Han,^{a,c} and Zhongping
Zhang^{a,b,d,*}

^aCAS Center for Excellence in Nanoscience, Institute of Intelligent Machines, Chinese Academy of Sciences, Hefei, Anhui 230031, China.

^bDepartment of Chemistry, University of Science and Technology of China, Hefei, Anhui 230026, China.

^cInstitute of Materials Research and Engineering, A-STAR, 3 Research Link, Singapore 117602.

^dState Key Laboratory of Transducer Technology, Chinese Academy of Sciences, Hefei, Anhui 230031, China.

E-mail: zpzhang@iim.ac.cn.

† These authors contributed equally to this work.

Contents

1. Regents and Instruments
2. Measurements of Quantum Yields
3. Structural Characterizations of Fluorescent Probe: Figures S1-S4
4. Reaction Mechanisms and Product Characterizations: Scheme S1, Figures S5-S11
5. Spectral Responses of Probe to •OH: Figures S12-S14
6. Spectral Responses of Probe to HClO: Figures S15-S17
7. Spectral Discriminations of •OH and HClO: Figures S18, S19, Table S1
8. Viability of Cells with Probes: Figure S20
9. Quantifications, Endogenous Co-localization, Scavenger Controls and Exogenous Co-localization of Cellular Imaging: Figures S21-S24
10. Control Experiments in Fluorescent Imaging of Living Zebrafish: Figures S25-S28

1. Reagents and Instruments

Reagents: Fluorescein, 2-[2-(2-chloroethoxy)ethoxy]ethanol, phorbol 12-myristate 13-acetate (PMA), MitoTracker Red CMXRos, mannitol, *N*-acetyl-L-cysteine (NAC) and NONOate were purchased from Sigma. FeSO₄, H₂O₂, NaClO, KO₂, NaNO₂, H₂SO₄, CH₂Cl₂, dimethylsulfoxide (DMSO), methanol, ethylene diamine tetraacetic acid disodium salt (EDTA) and *N,N*-dimethylformamide (DMF) were used as received from Shanghai Chemicals Ltd. EDTA-Fe²⁺ was prepared by mixing EDTA and FeSO₄. ROS/RNS were prepared as follows. Different concentrations of hydroxyl radicals (\bullet OH) in Fenton system were generated in situ by mixing different amounts of H₂O₂ into 1 mM FeSO₄. HClO was obtained by diluting aqueous NaClO with PBS buffer (pH 7.2). Singlet oxygen (¹O₂) was prepared by adding 1 mM NaClO into 1 mM H₂O₂. Superoxide (O₂^{•-}) was got by dissolving KO₂ in DMSO solution. Nitric oxide (NO) originated from the decomposition of 1 mM NONOate. Peroxynitrite (ONOO⁻) was obtained by mixing 1 mM NaNO₂ and 1 mM H₂O₂. The concentrations of NaClO were determined by measuring their UV spectra immediately before use.

Instruments: IR spectra were recorded with a Nicolet FT-IR Nexus 870 instrument (KBr disks) in the 400-4000 cm⁻¹ region. NMR spectra were performed on Bruker 400 MHz Ultrashield spectrometer and reported as parts per million (ppm) from TMS (δ). High-resolution mass spectra (HR-MS) were obtained using an Agilent Q-TOF 6540 mass spectrometer. UV-visible absorption spectra were measured with a Shimadzu UV-2550 spectrometer. Fluorescent spectra were recorded using Cary Eclipse fluorescence spectrophotometer. Fluorescent images were acquired on confocal microscope (Zeiss LSM 710), and the excitation wavelengths were 405, 488 and 633 nm.

2. Measurements of Quantum Yields

The fluorescence quantum yields (Φ_F) of FHZ, FOBA and F-TEG were determined using fluorescein (0.1 M NaOH, $\Phi_F = 0.95$) as the standard reference, according to the literature method.^{S1} The quantum yields were corrected as follows:

$$\Phi_s = \Phi_r \frac{A_r D_s}{A_s D_r}$$

where the s and r indices designate the sample and reference samples, respectively, A is the absorbance at λ_{ex} , and D is the integrated area under the spectrum.

3. Structural Characterizations of Fluorescent Probe

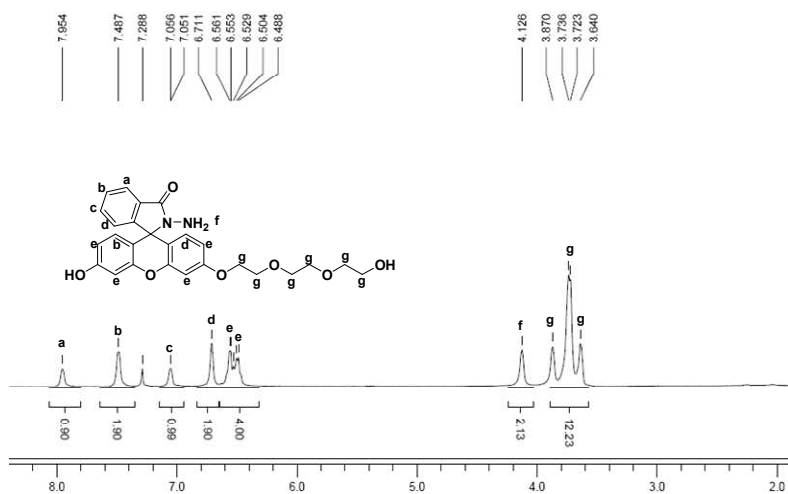


Figure S1. ¹H-NMR spectrum of FHZ.

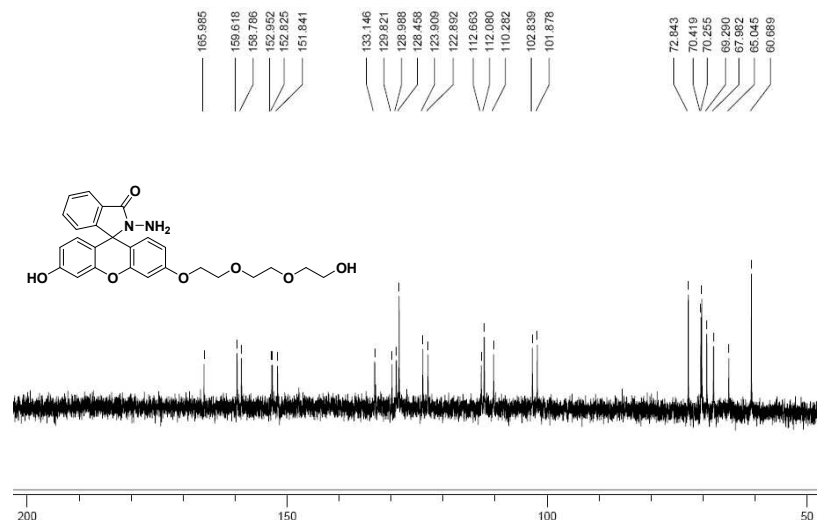


Figure S2. ^{13}C -NMR spectrum of FHZ.

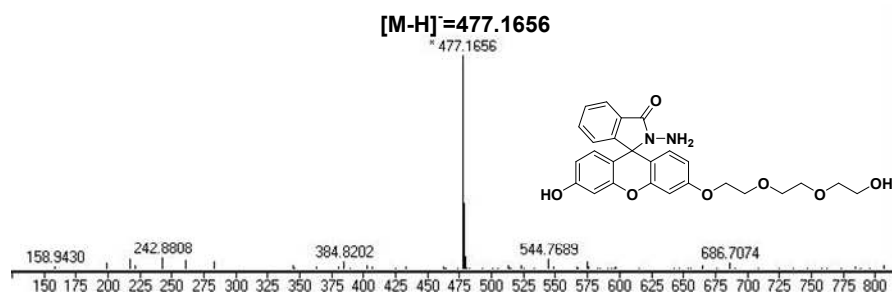


Figure S3. HR-MS spectrum of FHZ ($[\text{M}-\text{H}] = 477.1662$).

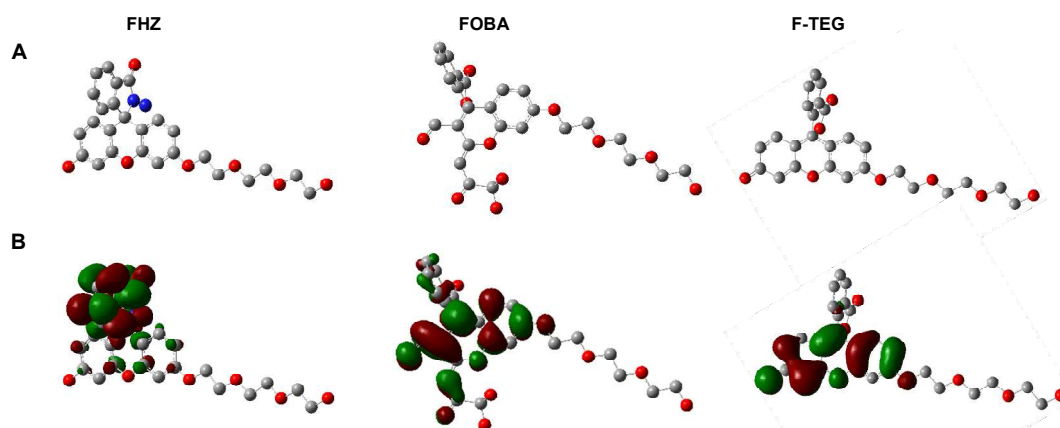
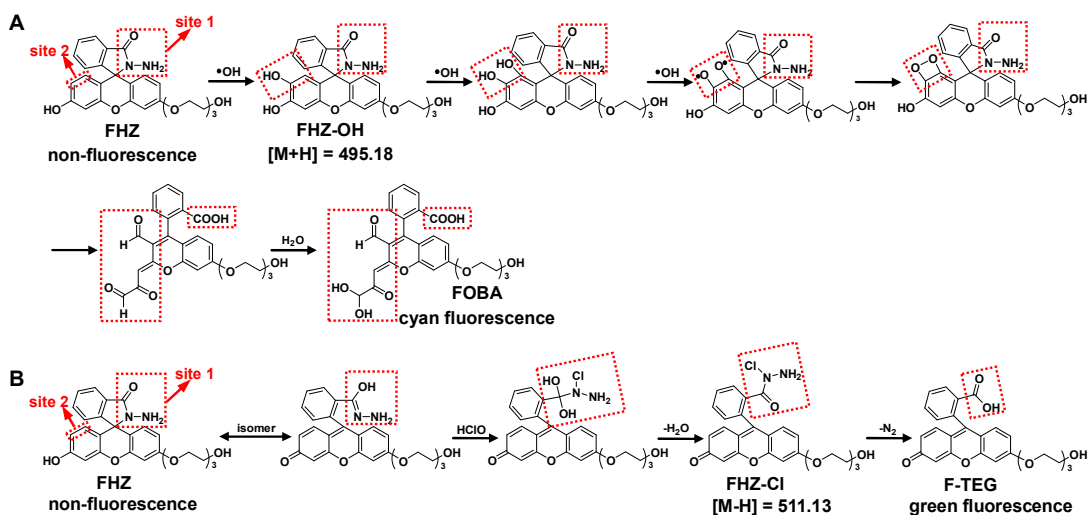


Figure S4. The optimal stereochemical structures (A) and electron cloud distribution (B) of FHZ, FOBA and F-TEG calculated by Gaussian 09 software at B3LYP/6-31G(d) level.

4. Reaction Mechanisms and Product Characterizations



Scheme S1. (A) Proposed mechanisms of sensing $\bullet\text{OH}$. At the site 2, $\bullet\text{OH}$ radicals rapidly react with aromatic rings of fluorescein group and form a stable intermediate FHZ-OH, which can continuously react with $\bullet\text{OH}$ and form a diphenol structure. The diphenol very easily reacts with $\bullet\text{OH}$ to form a double radical structure, because the acidic hydroxyl group (-OH) connected with aromatic ring is quite reactive. Then, the two single electronics of double radicals couple/form an extremely unstable four-membered peroxy ring, resulting in the opening reactions of the aromatic and five-membered rings.^{S2} The formed formyl group adjacent to the carbonyl group (C=O) is very unstable and combines a H_2O molecule to form the final product FOBA.^{S3} (B) Proposed mechanisms of sensing HClO . FHZ has an isomer with a C=N bond. Thus, the ring can be opened by the addition reaction of HClO with the C=N bond, resulting in a highly unstable intermediate product with two hydroxyl groups at the same carbon atom.^{S4} The following loss of a H_2O molecule forms another unstable intermediate FHZ-Cl. The lateral group of N-chloro amide is finally cleaved from the mother molecule, and then the final product F-TEG is formed. It should be noted that the studies on the reaction of $\bullet\text{OH}$ with FHZ do not find the intermediate product by only reacting at site 1 of the five membered ring (instead, through reaction at the site 2 first followed by the site 1 then). Therefore, this does not lead to the error in quantification of HClO when both $\bullet\text{OH}$ and HClO are existing in a system.

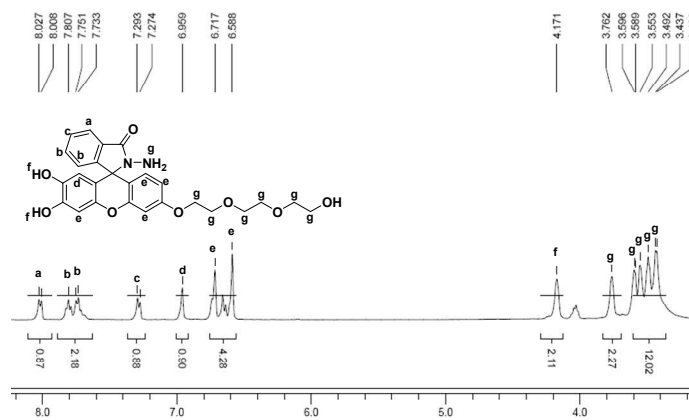


Figure S5. $^1\text{H-NMR}$ spectrum of FHZ-OH.

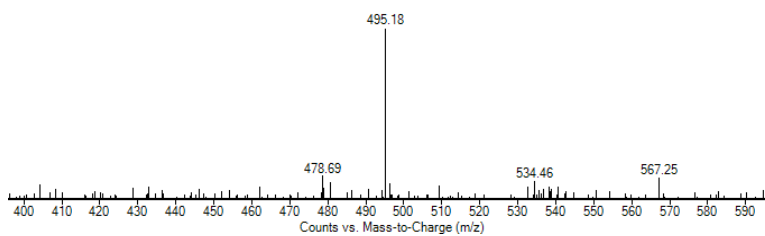


Figure S6. MS spectrum of FHZ-OH ($[\text{M}+\text{H}] = 495.18$).

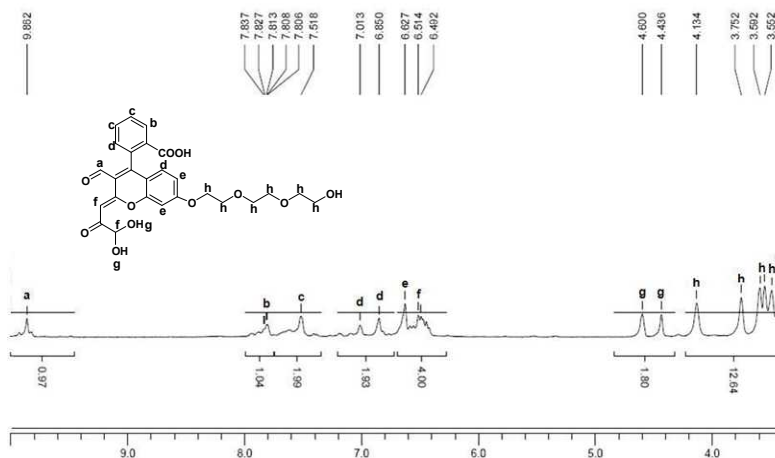


Figure S7. $^1\text{H-NMR}$ spectrum of FOBA.

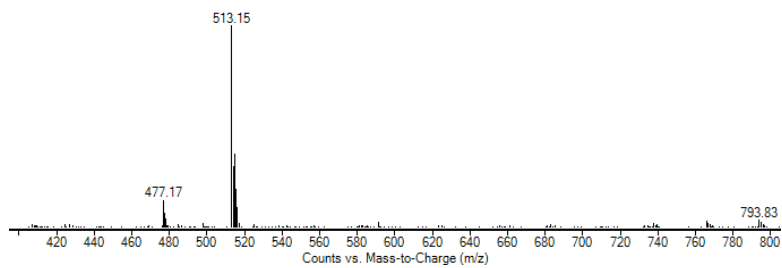


Figure S8. MS spectrum of FOBA ([M-H] = 513.15).

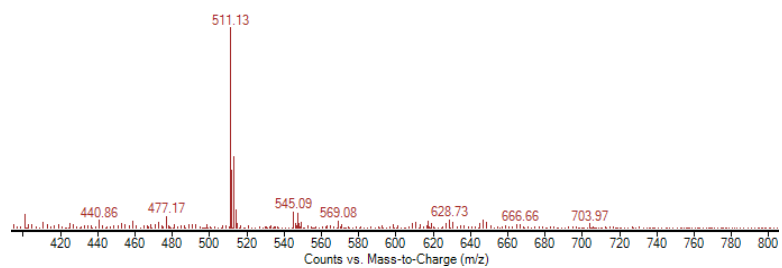


Figure S9. MS spectrum of FHZ-Cl ([M-H] = 511.13).

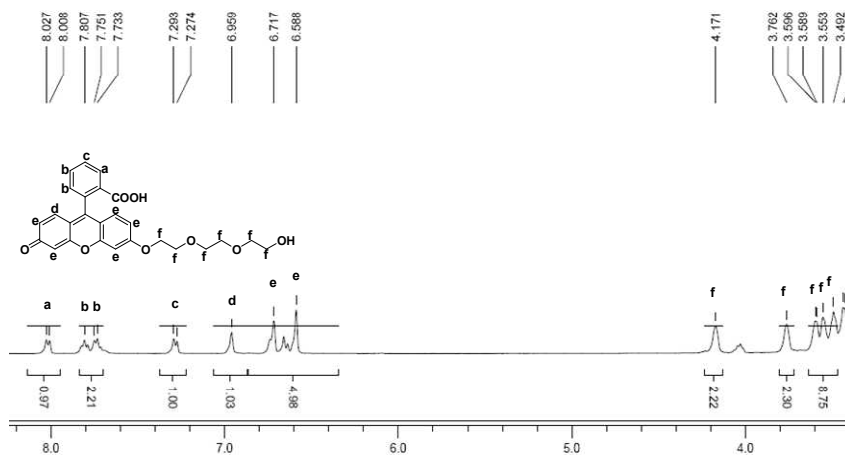


Figure S10. ¹H-NMR spectrum of F-TEG.

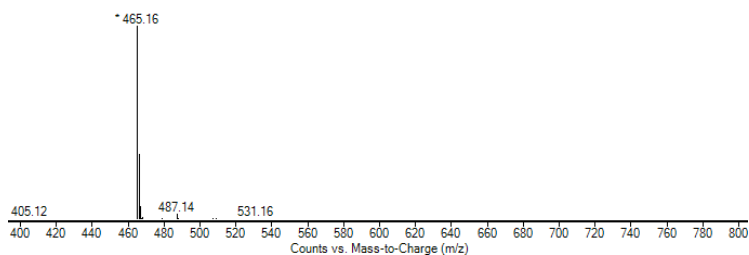


Figure S11. MS spectrum of F-TEG ($[M+H] = 465.16$).

5. Spectral Responses of Probe to $\bullet\text{OH}$

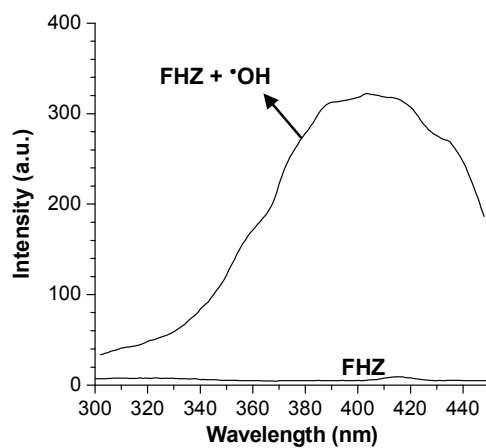


Figure S12. Excitation spectra of FHZ (10 μM) and FHZ (10 μM) + $\bullet\text{OH}$ (1 mM FeSO_4 + 1 mM H_2O_2) in PBS buffer. Here, the emission wavelength is fixed at 486 nm.

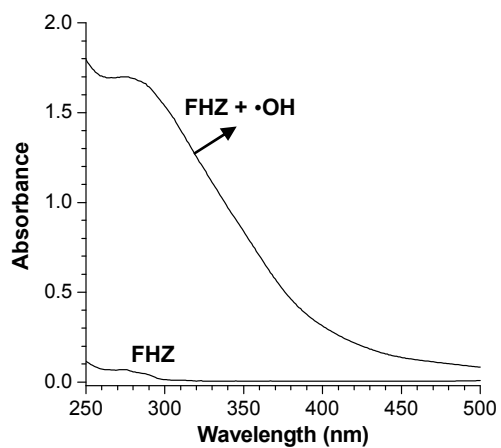


Figure S13. UV-vis absorption spectra of FHZ (10 μM) and FHZ (10 μM) + $\bullet\text{OH}$ (1 mM FeSO_4 + 1 mM H_2O_2) in PBS buffer.

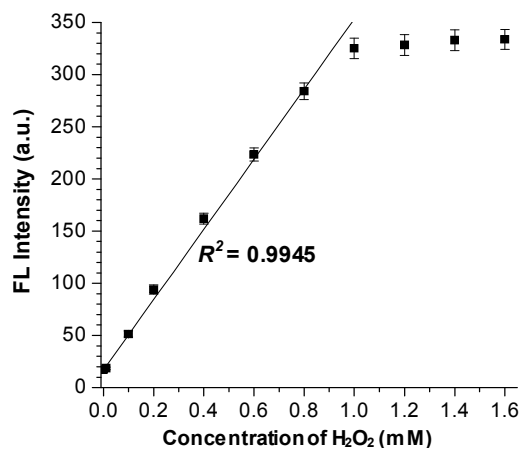


Figure S14. The titration curve was plotted by emission intensity at 486 nm versus H_2O_2 concentrations.

6. Spectral Responses of Probe to HClO

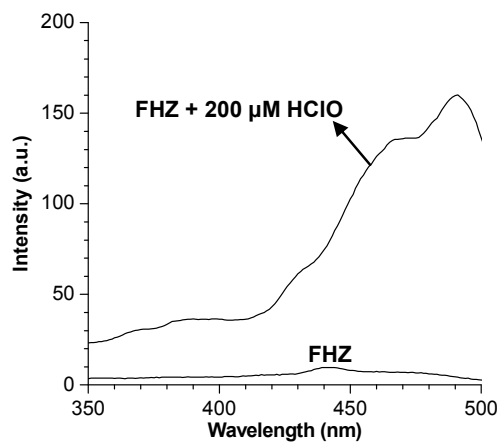


Figure S15. Excitation spectra of FHZ (10 μM) and FHZ (10 μM) + HClO (200 μM) in PBS buffer. Here, the emission wavelength is fixed at 520 nm.

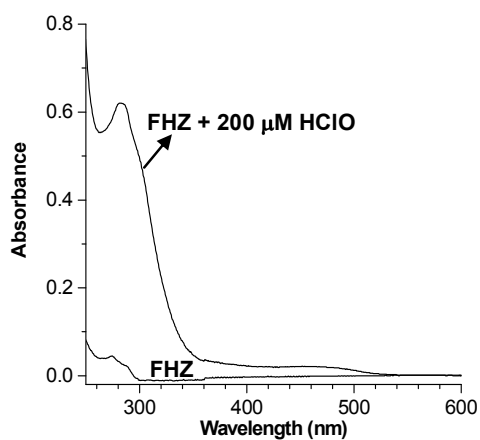


Figure S16. UV-vis absorption spectra of FHZ (10 μM) and FHZ (10 μM) + HClO (200 μM) in PBS buffer.

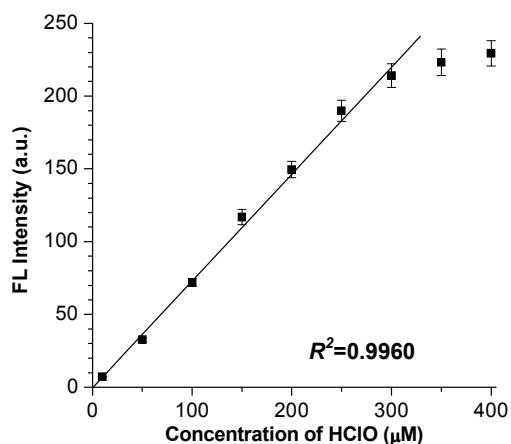


Figure S17. The titration curve was plotted by the emission intensity at 520 nm versus HClO concentrations.

7. Spectral Discriminations of •OH and HClO

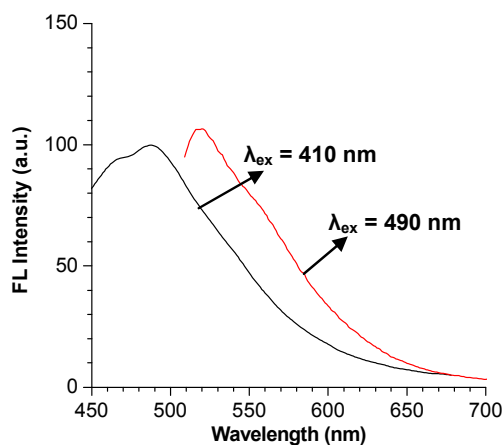


Figure S18. Fluorescent spectra of probe FHZ after simultaneously reacted with •OH and HClO in a mixing system. The resultant mixture was excited with 410 and 490 nm. The black curve represents the fluorescent response to •OH, and the red one is the fluorescent response to HClO.

Table S1. The quantum yields (Φ), molar extinction coefficients (ϵ) and fluorescent brightnesses (B) of FHZ, FOBA and F-TEG in aqueous solution.*

	FHZ	FOBA	F-TEG
Φ	0.01	0.42	0.34
ϵ_{410} ($M^{-1}\cdot cm^{-1}$)	300	12000	1000
B_{410} ($M^{-1}\cdot cm^{-1}$)	0.003	5.0	0.34
ϵ_{490} ($M^{-1}\cdot cm^{-1}$)	300	1300	7000
B_{490} ($M^{-1}\cdot cm^{-1}$)	0.003	0.55	2.4

* Φ is the quantum yield, and ϵ_{410} , ϵ_{490} , B_{410} and B_{490} represent the molar extinction coefficients and the fluorescence brightness at 410 and 490 nm, respectively. $B = (\epsilon \times \Phi) / 1000$. It is noted that the observed brightness in the fluorescent imaging largely depends on the spectral wavelength ranges of interest in the fluorescence collection windows we set. The difference in brightness together with the set collection windows (colors) provides the obvious spectral discriminations to $\bullet OH$ and $HClO$ (Figure S19).

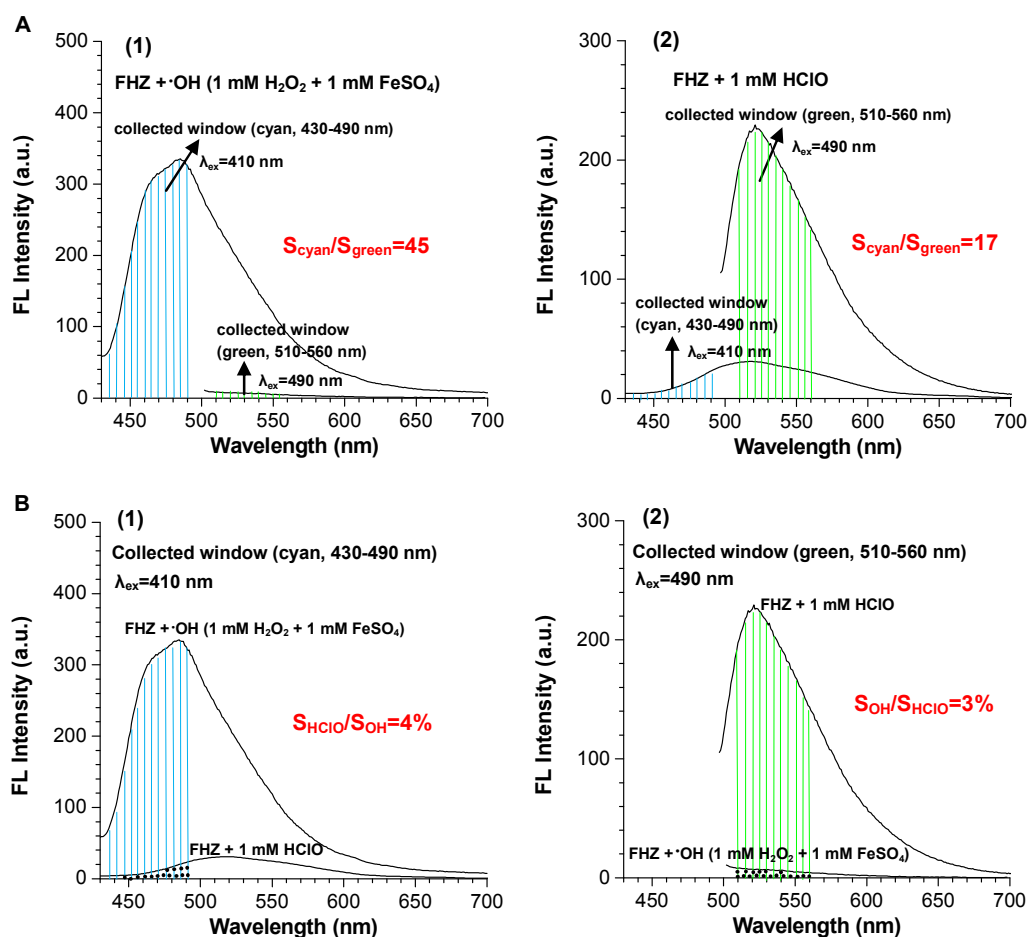


Figure S19. (A) The comparisons of fluorescence response of FHZ to ROS at the different excitation wavelengths and collection windows: (1) •OH (1 mM H₂O₂ and 1 mM FeSO₄) with the excitations at 410 and 490 nm and the collection at cyan (430-490 nm) and green (510-560 nm) windows, respectively; (2) HClO (1 mM) with the excitations at 410 and 490 nm and the collection at the same cyan and green windows, respectively. (B) The comparisons of fluorescence response of FHZ to ROS at the identical excitation wavelength and collection window: (1) cyan channel (excitation at 410 nm, collection in 430-490 nm); (2) green channel (excitation at 490 nm, collection in 510-560 nm).

Analysis: Figure S19 shows the detailed examinations on the spectral profiles and intensities in the presence of •OH or HClO upon excitation at the two different wavelengths and then collection in two different windows (cyan and green). In the presence of •OH, the fluorescence intensity collected from cyan channel is about 45 times of that from green channel owing to the two different excitation wavelength used (Figure S19-A1). In the case of HClO, the fluorescence intensity collected from green channel is about 17 times of that from cyan channel (Figure S19-A2). On the other hand, Figure S19-B shows the interference of spectral overlap in the case of co-existing •OH and HClO. For the detection of •OH with the excitation at 410 nm, the spectral interference of HClO to the

result is only about 4%. For the detection of HClO with the excitation at 490 nm, the spectral interference of $\bullet\text{OH}$ to the result is only about 3%. Therefore, under the set experimental conditions, these interferences incurred by the spectral overlap are completely acceptable in the error range.

8. Viability of Cells with Probes

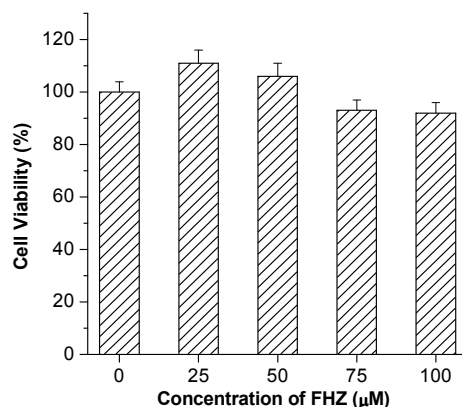


Figure S20. Viability of HeLa cells in the presence of the probe as measured by using MTT assay. HeLa cells (10^5 cell/mL) were dispersed with replicate 96-well microtiter plates to a total volume of $200 \mu\text{L well}^{-1}$. Plates were maintained at 37°C in 5% $\text{CO}_2/95\%$ air incubator for 12 h. The cells were incubated for an additional 12 h with the probe with different concentrations of 25, 50, 75 and $100 \mu\text{M}$. Subsequently, 5 mg/mL MTT (3-(4,5-dimethylthiazol-2-yl)-2,5-diphenyl tetrazolium bromide) in PBS was then added in each well, followed by further incubation for 4 h at 37°C . The absorbance was measured at 490 nm in TRITURUS microplate reader. The error bars represent the mean errors from the results of 3 tests.

9. Quantifications, Endogenous Co-localization, Scavenger Controls and Exogenous Co-localization of Cellular Imaging

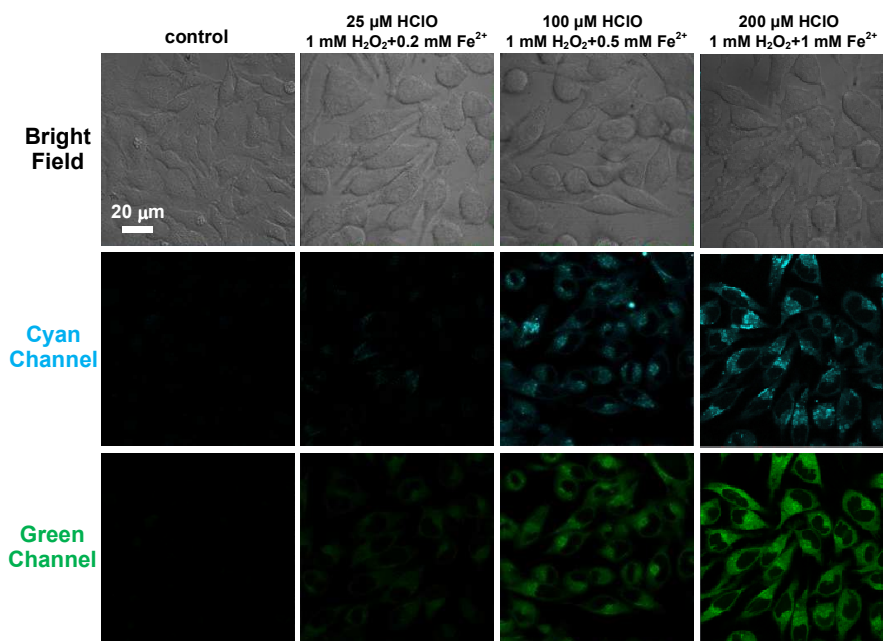


Figure S21. Dose-dependent fluorescent images of HeLa cells from cyan channel (excited at 405 nm and collected at 430-490 nm) and green channel (excited at 488 nm and collected at 510-560 nm). HeLa cells were incubated in 100 μM probe FHZ, and then treated with HClO, H_2O_2 and EDTA- Fe^{2+} in order. The concentrations of the HClO, H_2O_2 and EDTA- Fe^{2+} were indicated at the top of the image columns. Before the fluorescent imaging, each treatment of cells kept 30 min, and then the cells were washed with PBS buffer three times.

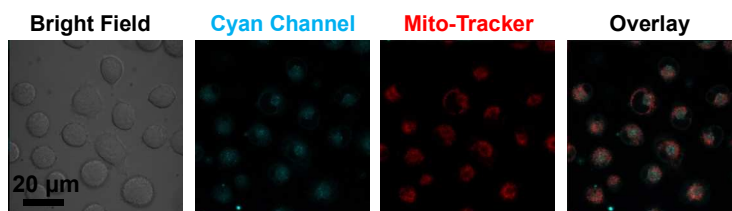


Figure S22. The visualization of endogenous $\bullet\text{OH}$ in HeLa cells by the stimulation of PMA and the co-localizing overlay images with mito-tracker dye (MitoTracker Red CMXRos). HeLa cells were incubated with 50 μM FHZ for 30 min, and then treated with 2 $\mu\text{g}/\text{mL}$ PMA for 4 h and 5 μM MitoTracker Red for another 30 min. The co-localization coefficient is 0.65.

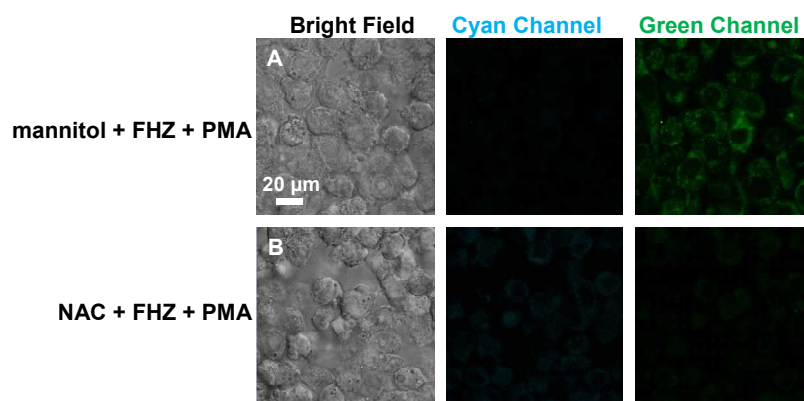


Figure S23. Confocal fluorescent images of RAW 264.7 macrophages sequentially treated with ROS scavengers, FHZ and PMA. (A) RAW 264.7 macrophages were first incubated in 100 mM mannitol (a scavenger for $\bullet\text{OH}$) for 30 min and then treated with 100 μM FHZ for 30 min and 2.0 $\mu\text{g}/\text{mL}$ PMA for another 4 h. (B) RAW 264.7 macrophages were first incubated in 10 mM NAC (a scavenger for HClO and $\bullet\text{OH}$) for 30 min, and then treated with 100 μM FHZ for 30 min and 2.0 $\mu\text{g}/\text{mL}$ PMA for another 4 h.

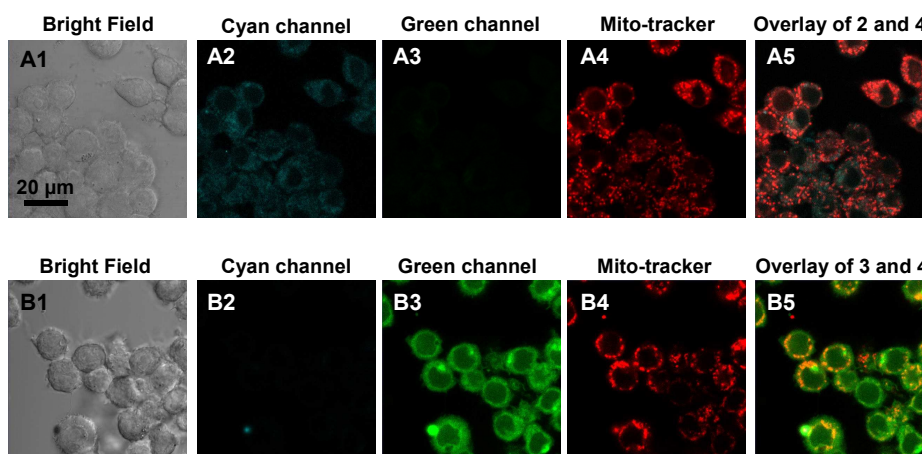


Figure S24. Visualization of exogenous $\bullet\text{OH}$ and HClO in RAW 264.7 macrophages and co-localizing overlay images with mito-tracker dye (MitoTracker Red CMXRos). (A) RAW 264.7 macrophages were incubated with 100 μM FHZ for 30 min and then treated with 1 mM H_2O_2 for 30 min, 1 mM EDTA-Fe^{2+} for 30 min and 5 μM MitoTracker Red for another 30 min. (A1) Bright field image of RAW 264.7 macrophages. (A2) Fluorescent image of RAW 264.7 macrophages from cyan channel (excited at 405 nm and emission collected at 430-490 nm). (A3) Fluorescent image of RAW 264.7 macrophages from green channel (excited at 488 nm and emission collected at 510-560 nm). (A4) Fluorescent image of RAW 264.7 macrophages from the channel (excited at 633 nm and emission collected at 650-700 nm) for MitoTracker Red CMXRos. (A5) Overlay of (A2) and (A4). (B)

RAW 264.7 macrophages were incubated with 100 μM FHZ for 30 min and then treated with 200 μM HClO for 30 min and 5 μM MitoTracker Red for another 30 min. (B1) Bright field image of RAW 264.7 macrophages. (B2) Fluorescent image of RAW 264.7 macrophages from cyan channel. (B3) Fluorescent image of RAW 264.7 macrophages from green channel. (B4) Fluorescent image of RAW 264.7 macrophages from the channel for MitoTracker Red CMXRos. (B5) Overlay of (B3) and (B4).

10. Control Experiments in Fluorescent Imaging of Living Zebrafish

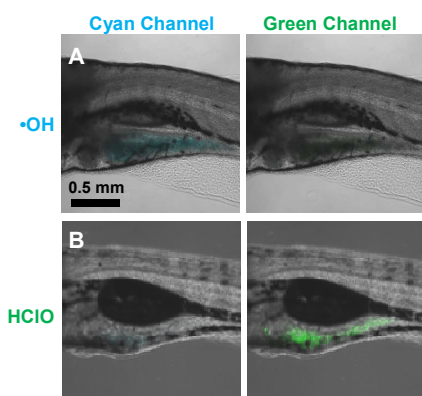


Figure S25. Determinations of exogenous ROS in living zebrafish. The seven-day old zebrafish after fertilization were cultured in 50 μM aqueous FHZ for 30 min at 28 $^{\circ}\text{C}$ and then raised in oxygen-dissolving water. (A) The visualization of exogenous $\bullet\text{OH}$ in the living zebrafish treated further with 100 μM H_2O_2 and 100 μM EDTA-Fe^{2+} in order to supply $\bullet\text{OH}$ for 30 min. (B) The visualization of exogenous HClO in the living zebrafish treated further with 50 μM HClO for 30 min. In Figure 6A, the observations of cyan and green signals from endogenous ROS needed the time period of 3 h after the addition of probe FHZ.

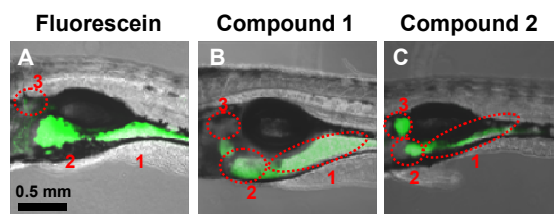


Figure S26. Confocal fluorescent images of living zebrafish incubated in the three similar dye solutions: (A) 50 μM fluorescein, (B) 50 μM compound 1 and (C) 50 μM compound 2 from green channel (regions: 1, intestine; 2, liver; 3, pronephros).

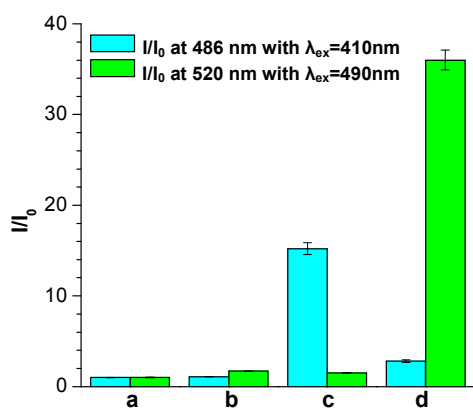


Figure S27. The fluorescent responses (I/I_0) of FHZ (10 μM) to the fresh zebrafish lysates (2 mL): (a) probe FHZ only; (b) FHZ + zebrafish lysates; (c) FHZ + zebrafish lysates + $\bullet\text{OH}$ (1 mM H_2O_2 +1 mM FeSO_4); (d) FHZ + zebrafish lysates + HClO (1 mM). The cyan and green fluorescences were excited with 410 and 490 nm, respectively. The aqueous FHZ with zebrafish lysates was incubated at 28°C for 4 h. The error bars represent the mean errors from the results of 5 tests.

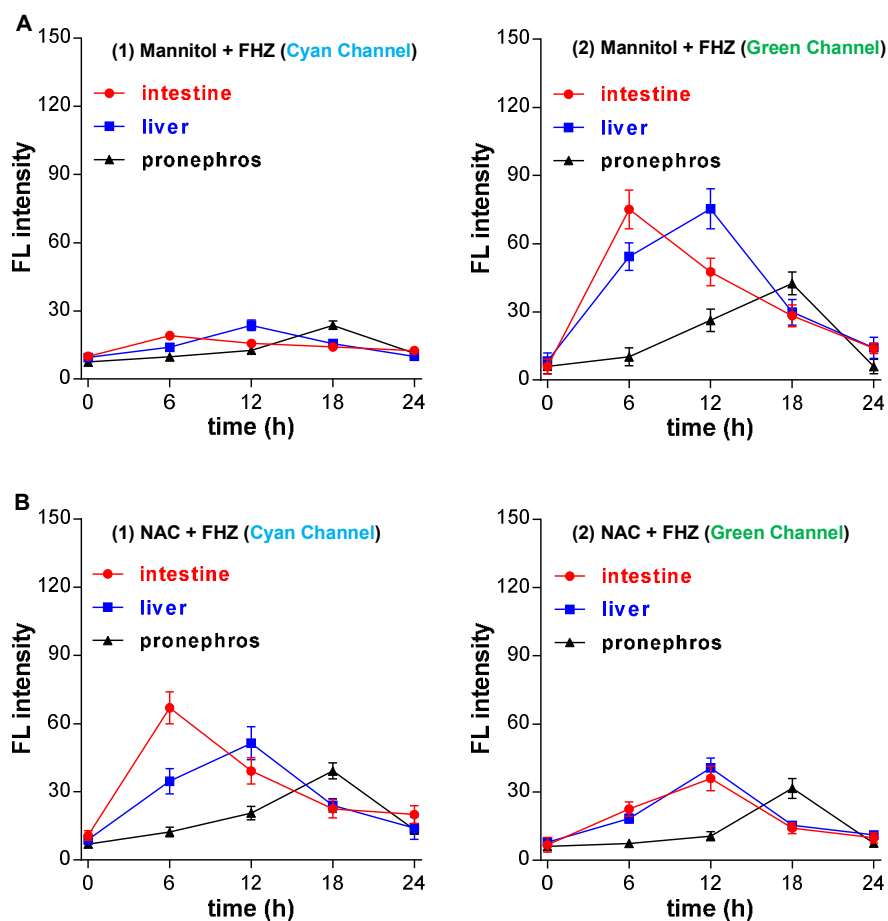


Figure S28. The time-dependent mean fluorescence intensities from cyan and green channels in different zebrafish organs in the control experiments. (A) The zebrafish were incubated in 10 mM mannitol for 30 min and then cultured in 50 μ M FHZ for another 30 min. After the two-step treatments, the zebrafish were raised in water and the time was set as zero time point. (B) The zebrafish were incubated in 1 mM NAC for 30 min and then cultured in 50 μ M FHZ for another 30 min. After the two-step treatments, the zebrafish were raised in water and the time was set as zero time point. The fluorescence intensities were the integrals of fluorescence collected from the whole organs of intestine, liver and pronephros. The mean intensity was obtained from six zebrafish and the error bars represent standard deviation (\pm SD).

Reference

- (S1) Mataga, N.; Kaifu, Y.; Koizumi, M. *Bull. Chem. Soc. Jpn.* **1956**, *29*, 465-470.
- (S2) Ou, B.; Hampsch-Woodill, M.; Prior, R. L. *J. Agric. Food Chem.* **2001**, *49*, 4619-4626.
- (S3) Eftekhari-Sis, B.; Zirak, M.; Akbari, A. *Chem. Rev.* **2013**, *113*, 2958-3043.
- (S4) Zhang, Z.; Zheng, Y.; Hang, W.; Yan, X.; Zhao, Y. *Talanta* **2011**, *85*, 779-786.